International Journal for Housing Science and Its Applications
Publish August 10, 2025. Volume 46, Issue 4 Pages 1755-1764

https://doi.org/10.70517/ijhsa464153

Computer-Aided Modeling and Analysis of Biomechanical Characteristics of the Lower Limb in Jumping Movements

Haixu Wang[1,*]
[1] School of Intelligence and Engineering, Shenyang City University, Shenyang, Liaoning, 110112, China
Corresponding authors: (e-mail: onepiece521521@163.com).

Abstract In this paper, a multi-rigid-body system dynamics method, combined with OpenSim model, was used to experimentally test and simulate and analyze 100 subjects. Visual3D was used to verify the validity of the OpenSim model. The biomechanical characteristics of the lower limbs in jumping exercise were analyzed by intergroup comparisons of kinematic data, electromyographic signals of the muscles, and center of mass displacement parameters. There were significant differences between group I and group II in the knee joint angle and angular velocity ($P<0.05$). The muscles that exerted the most force during jumping were the tibialis anterior muscle and the rectus femoris muscle in group I. The muscles that exerted the most force in the process of jumping were the tibialis anterior muscle and the rectus femoris muscle in group II. In group II, the medial head of gastrocnemius muscle and rectus femoris muscle exerted the most force, and the excessive tension of the supporting leg muscles was one of the main reasons for the poor jumping effect. The representatives of group I all had a free time of more than 0.7s, and the displacement of Z-axis vertical direction was more than 0.7m, which verified that the full utilization of rapid force in the stomping stage played a decisive role.

Index Terms multi-rigid body system dynamics, OpenSim model, jumping movement, biomechanical properties

I. Introduction

Jumping to the ground is a common action in sports, and it is also one of the common actions that can easily cause sports injuries. When the lower limb touches the ground during jumping, abnormal kinematic and kinetic manifestations such as a decrease in knee flexion angle and moment, and an increase in ground reaction force may increase the tension on the anterior cruciate ligament [1]-[3]. Changes in these biomechanical indicators have also been used as an important basis for assessing the risk of non-contact ACL injuries [4].

It is always known that the achievements in human motion analysis followed the development of modeling and simulation methods for musculoskeletal dynamics and motion control [5], [6]. With today's powerful computational support, increasingly complex large-scale models are being constructed to produce realistic simulations of motion, many of which can also be used across a wide range of industries [7]. Inverse dynamics techniques applied to biomechanical models of the human body are widely used in the fields of orthopedics, ergonomics, sports science, and medical rehabilitation [8], [9]. They aim to quantitatively assess the muscular forces and internal loads acting on bones and joints in the human body during various activities, and by gaining insight into how muscular forces interact to produce coordinated movements of body parts, a deeper understanding of the underlying neural control can be gained [10]-[13].

Traditional studies have analyzed movement techniques and explored the effects of force on performance and achievement based on quantitative descriptive comparisons of kinematic and kinetic parameters, while an objective evaluation of the role of muscles in movement cannot be achieved [14]-[16]. Sports biomechanics modeling and simulation technology, an emerging research tool, can effectively evaluate the relationship between muscle function and sports performance in jumping to improve sports performance, or avoid the risk of jumping sports injuries by focusing on abnormal joint kinematics, which plays an important role in the field of sports [17]-[20].

In this paper, we first establish the equations of motion for the lower limb system based on the multi-rigid body system dynamics approach, combined with methodological foundations such as Kane's method. The typical stages of jumping movement are decomposed as the entry point of biomechanical analysis. OpenSim muscle mechanics model and musculoskeletal model are introduced to integrate multi-physics field information such as muscle activation, joint constraints and ground reaction force. Real motion data were obtained through experimental tests with 87 subjects. The Visual3D results were compared with the OpenSim simulation results in terms of similarity within the ICC group to evaluate the performance level of the model. Comparatively analyze the biomechanical indexes of different levels of jumpers to reveal the key biomechanical differences.

II. Design of a methodology for analyzing the biomechanics of the lower extremity in jumping sports

As a core technical movement in many sports such as track and field, basketball and volleyball, jumping is closely related to the biomechanical properties of the lower limbs. As the main support and power source of human movement, the synergistic mechanism of muscles, bones and joints in the jumping process directly affects the jumping height, stability and efficiency of the movement, and it is also a key research direction for the prevention of sports injuries.

II. A.Methods for studying the dynamics of multi-rigid body systems

With the development of technology, the dynamics of multi-rigid-body systems has developed a variety of distinctive systems of methods, all of which have the feasibility of being applied to computer calculations. The differential equations of dynamics in many systems are no longer just higher-order nonlinearities, but can be constructed and computed by electronic computers. In the following, some of the landmark technical methods in the study of dynamics of multi-rigid-body systems will be introduced:

(1) Graph theoretic approach: using the graph theoretic approach, the graph theoretic knowledge of mathematics can be applied to multi-body system dynamics so as to determine the topological correlations of the structural diagram of the system, and the correlation matrix and channel matrix techniques can be utilized to depict the internal structure of the system and the connectivity correlations.

(2) Maximum number of coordinates method: Through the maximum scale coordinate system method, it is possible to use the six positions of each rigid body in the system as a coordinate system, and use Lagrange operators and differential equations associatively to construct a Jacobi matrix of constrained variables, which leads to the dynamical process.

(3) Lagrange's method: Lagrange's method is a method used to represent the coordinates of the mass points in a system of mass points, which expresses the coordinates of each mass point in the system of mass points as an independent coordinate, which depends on the size of each mass point in the system of mass points, and is usually represented by an independent parameter $q_1, q_2 \cdots q_j$ and t, i.e.:

$$r_i = r_i(q_1, q_2 - ..q_j, t) \tag{1}$$

In the Lagrangian coordinate system, $q_1, q_2 \cdots q_j$ are called Lagrange generalized coordinates, which do not just represent distances, they may also be angles or some natural physical quantity. In the case of geometric constraints, the number of these coordinates is the number of degrees of freedom, and they can be used to derive the Lagrangian equations, i.e.:

$$\frac{d}{d_t}\left(\frac{\partial T}{\partial \dot{q}_j}\right) - \left(\frac{\partial T}{\partial q_j}\right) = Q_J \quad (j = 1, 2, \ldots, i) \tag{2}$$

In Eq. q_j are generalized coordinates; $\dot{q}_j$ generalized velocity; $T = \sum_{i=1}^{n}\left(\frac{1}{2} m_i r_i^2\right)$ is the kinetic energy of the system of masses; $\left(\frac{\partial}{T}\partial q_i\right)$ is the generalized momentum; Q_J is a generalized force (generally excluding binding forces) and is a function of $q_j(q_1, q_2 \ldots q_i)$. And the magnitude of $Q_J \delta q_j$ is the magnitude of work, so the magnitude of Q_J will vary with the choice of q_j. q_j can be a force, a moment or some other physical quantity.

Since the generalized force Q_J in the Lagrange equations generally does not include the constraint counterforce, this greatly simplifies the mathematical modeling of human motion. In the human body modeled as a multi-rigid body, the constraint counterforce is usually unknown, and thus we are able to solve the Lagrange equations much more easily.

Based on the principle of virtual work and D'Alembert's principle, the introduction of a generalized coordinate system of scalar structures, basic physical quantities such as energy and work, and a purely geometric approach allows the dynamical equations to be based on a systematic mathematical theory, which greatly narrows down the influence of the constraint forces and makes the analysis of vector mechanics easier and more effective. The advantage of the pull equations is that if the dynamics Q_J of a given system of masses and the forces q_j acting on it are known, they should be used to express the pull equations of these systems of masses.

(4) Kane's Method: The Kane's method is a method used to compute the dynamics of a system by projecting the true and inertial forces directly into specific directions to eliminate the ideal constraint forces. This method is adapted

to both integral and incomplete control systems. Its basic idea is to describe the operation of a system by using generalized velocities instead of the traditional coordinate system.

A prime in the prime system $P_i(1,2,3...,n)$ has a velocity $v_i = \dot{r}_i$ that can be uniquely expressed as a linear combination of the pseudo-velocities $U_\alpha(\alpha = 1,2,\ldots,s)$ as:

$$v_i = \sum_{i=1}^{s}\sum^{n} v_i^{(\alpha)} U_\alpha + v_i^{(0)} \tag{3}$$

where we call U_α the pseudo-velocity and $v_i^{(\alpha)}$ the α bias velocity of the i th prime since there are no corresponding generalized coordinates. In practical calculations, the partial velocities are usually expressed as base vectors or combinations of base vectors.

Taking the velocity variances for each term, we can derive the velocity variances for each mass point, which can be independently expressed as δU_α.

$$\delta v_i = \sum_{i=1}^{s}\sum^{n} v_i^{(\alpha)} \delta U_\alpha \tag{4}$$

This can be obtained using the imaginary power principle:

$$\sum_{\alpha=1}^{s}\left(\sum_{i=1}^{n} F_i \cdot v_i^{(\alpha)} + \sum_{i=1}^{n} F_i \cdot v_i^{(\alpha)}\right)\delta u_\alpha = 0 \tag{5}$$

If $\tilde{F}_\alpha = \sum_{i=1}^{n} F_i \cdot v_i^{(\alpha)}$ is regarded as a generalized active force, then $\tilde{F}_\alpha^* = \sum_{i=1}^{n} F_{I_i}^* \cdot v_i^{(\alpha)}$ is then the generalized inertial force, and $F_i^* = -m_i \ddot{r}_i$ denotes the inertial force of the prime P_i.

$$\tilde{F}_\alpha + \tilde{F}_\alpha^* = 0(\alpha = 1,2,\ldots,s) \tag{6}$$

The inference of Kane's equation is more concise than that of the pull-type differential equation, especially when n is large, and its inference steps are easier, however, the physics of Kane's equation becomes more complicated because it invokes the concepts of the imaginary rate, partial rate, plant generalized driving force, and extensive inertia force. The problem of insufficient accuracy of sports biomechanics instrumentation in the force measurement session leads to test results that do not reflect the true regularity of human movement, in addition, theoretical simulations lack a comprehensive consideration of the biomechanical situation in human movement.

Therefore, in the application of human body research, the dynamics analysis simulation should be combined with experiments according to the differences between different human bodies in order to provide more accurate initial motion conditions and boundary constraints, and at the same time, it can also reflect the actual situation of human body motion more realistically, so as to better realize the simulation practice of human body motion.

In this paper, we use ADAMS to analyze the multi-body dynamics of the human body, and study the establishment of equations using the Lagrange multiplier method, which is a mathematical method used to solve constrained optimization problems in analytical mechanics. By this method, we can construct the systematic equations of motion of the human lower limb to describe its dynamic behavior during motion. Specifically, we can use the Lagrange multiplier method to consider the interactions between the muscular and skeletal systems of the human lower extremity. This process needs to take into account the effects of gravity and other external forces on the lower limb, as well as factors such as muscle contraction and changes in joint angles.

$$\frac{d}{d_t}\left(\frac{\partial T}{\partial \dot{q}}\right)^T - \left(\frac{\partial T}{\partial q}\right)^T + \varphi_q^T \rho + \theta_q^T \mu = Q \tag{7}$$

Fully constrained equations:

$$\varphi(q,t) = 0 \tag{8}$$

Among them, T: kinetic energy of the system, Q: system generalized coordinate array, ρ: the Raschner multiplicative sublattice corresponding to the complete constraints, μ: corresponds to the Raschner multiplicative sublattice with incomplete constraints;

Rewritten in general form as follows;

$$F(q,\mu,\dot{u},\lambda,t)=0 \tag{9}$$

$$\phi(q,t)=0 \tag{10}$$

$$G(u,\dot{q})=0 \tag{11}$$

where, q : generalized velocity array, λ : column of forces, F : system dynamics differential equations, G : incomplete constraint equation array, $\varnothing$: array of complete constraint equations.

II. B.Biomechanical analysis of typical jumping movements

II. B. 1) Jumping phase

This phase, which can be divided into the buffer phase and the stomping and stretching phase, is quite critical, and the purpose of this phase is to exert a force on the ground by the foot through the coordinated action of all parts of the body, so that the center of mass of the body rises to a certain height and obtains a certain amount of rotational energy, which is directly related to the high quality of the later action can be accomplished.

(1) Buffer phase

The cushioning phase of the jump is the process in which the athlete's starting leg begins to flex the knee to cushion it after the braking forward stance of the starting leg, and finally reaches the maximum angle of knee flexion. Meanwhile, analyzing from the biomechanical point of view, according to the impulse-momentum theorem, the integral of the changing force with respect to time determines the final momentum of a mass: the special boundary of the integral of $\int Fdt=mV$ determines the change of momentum from the beginning moment (t_0) to the final moment (t_1), i.e., $\int_0^1 Fdt+mV_0=mV_1$ At the end of the buffer, the body begins to move upward at $V_i=0$, and thus $\int_0^1 Fdt=-mV_0$, which means that the greater the initial velocity at the start of the buffer, the greater the integral of the variable force with time, the more the muscle is fully elongated at the end of the buffer, and the force generation effect is significantly better than that of the squat jump without buffer. From the video analysis, it can be seen that the athletes will take a small step forward with the left foot before jumping, and then immediately land on the ground with both legs to start the cushioning of the jump, which also makes the initial velocity of the cushioning become larger, and thus produces a better jumping effect.

(2) Stirrup phase

The stirrup-off time phase refers to the time period from the beginning of the body's knee-bending cushioning center of mass dropping to the lowest to the moment when the body's feet leave the ground. Through video analysis, at the end of the cushioning phase, the athlete's body posture is not completely oriented in the forward direction, but rather there is a tilt and twist to the side and back, accompanied by a backward shift of the body's center of mass and an eccentric force generated on the foot to the diagonal backward direction, which produces three effects: a vertical movement of the center of mass, a horizontal movement of the center of mass, and the rotation of the body around the longitudinal and transverse axes that pass through the center of mass. First we analyze the biomechanical factors that affect the height of the rise of the human center of mass. Since after the jump the body is only affected by the downward gravitational acceleration, we can determine the entire vertical displacement of the center of mass using the uniformly accelerated motion equation. Using the formula: $V_f^2=V_i^2+2as$, it is known that the vertical component of the airborne velocity, (V_j), ends up being 0, as well as that the direction of the gravitational acceleration is negative, so we get:

$$S=V_i^2/2g \tag{12}$$

Here V_i is the initial vertical component of the maximum velocity at the time of the jump, which we rename V_{To} for the sake of analysis, as well as S is equal to the vertical displacement of the vacated air, and in order to obtain the V_{To}, the work has to be done in the stage of the stirrups stretching before the departure from the ground, and, according to the formula: $\int Fds+\frac{1}{2}mV_i^2=\frac{1}{2}mV_{To}^2$, and V_i is 0 at the end of the cushioning to start the stirrup reach, so the equation can be rewritten as:

$$V_{To}^2=\left(\frac{2}{m}\right)/Fds \tag{13}$$

At the same time:

$$F = F_z - mg \tag{14}$$

Substituting Eq. (13)(14) into Eq. (12) yields:

$$S = \left(\frac{2}{m}\right)\int (F_z - mg)ds / 2g \tag{15}$$

Since m and g are constants, the above equation clearly shows that there is only one variable that determines the height of the rise of the center of mass, i.e., the integral of the upward force with respect to the vertical displacement of the center of mass in the stirrup phase. Therefore, the height reached in a jump is determined by the amount of force that can be generated by the muscles in the stirrup phase and the height of the center of mass at the moment it leaves the ground. The ability of the muscles to generate force is related to the physiological condition of the athlete, as well as to the quality of the cushioning and the completion of the arm swing technique. The displacement of the center of mass, on the other hand, is related to the degree of extension of the body segments, especially the hip and knee joints.

II. B. 2) Emptying phase

The vacating phase is the whole process starting from the moment of stomping off the ground to the moment of landing again, and includes two parts: turning and bending the body to split the legs or straight body to vacate. There are two main mechanical principles that cannot be violated in the process of human vacating. The first is that the angular momentum generated during the jump remains constant in the air, and the aerial maneuver is affected by only one external force, gravity. The second mechanical principle is that any muscular force F and the joint moments M generated by F are internal forces to the system and they obey the law of action and reaction, so that there is no change in the angular momentum of the whole body. The main technical features of the rotational movement are rational control of the body posture, reduction of the radius of rotation to reduce the rotational inertia and increase of the angular velocity, which facilitates the rotation of the body.

II. C. OpenSim-based biomechanical analysis of human lower limbs

II. C. 1) Muscle mechanics modeling

Muscles, as drivers of human movement, are the basis of human biomechanics research, and the OpenSim muscle model is built based on the Hill model. The tendon complex consists of 3 components; the contractile element (CE), the parallel element (PE) and the serial element (SE). The muscle force produced is a function of 3 factors; muscle activation value, normalized length per unit and normalized velocity per unit. The functions describing the force produced by the muscle as the length changes are called the active length curve (AL) for the contractile element and the passive length curve (PL) for the parallel element. The principle of the modified Hill model is shown in Fig. 1. In the figure, $\alpha_M, L_M, L_T, L_{MT}$ are muscle fiber contraction angle, muscle fiber length, tendon length, and muscle-tendon length, respectively.

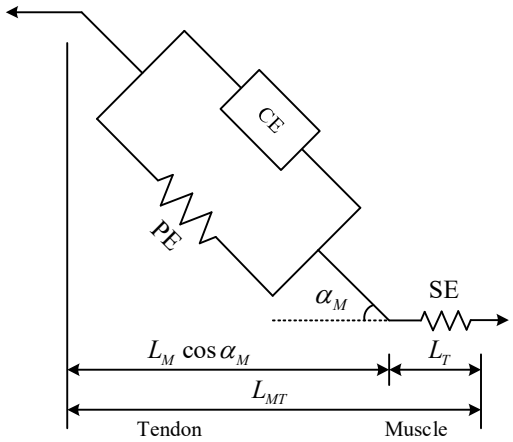

Figure 1: Improved Hill muscle model

II. C. 2) OpenSim musculoskeletal modeling

The OpenSim musculoskeletal model is used to represent a complex dynamical system of rigid bodies, joints, and muscles in the form of a text file consisting of a body, joints, forces, constraints, and controllers. The body is the

main bones of the human body with geometric and inertial properties, the relative motions between the bones are coupled by joints and their constraints, and the forces include internal forces from muscles and ligaments as well as external forces interacting with the ground. In addition, the musculoskeletal model is accompanied by a number of marker points to identify the location of the limb motion information acquisition points.

II. C. 3) Mode of obtaining plantar pressure

Ground reaction force is an important external motion load data required for human biomechanical analysis based on OpenSim, and currently the plantar pressure data are mainly acquired by force plates and other measurement tools to describe the ground reaction force on the sole of the foot. Different brands of force plates and sensors of different types and installation locations of different measurement methods, this paper to Ertec's Bertec6 component load sensor force plate as an experimental tool to illustrate the acquisition of plantar pressure, plantar pressure force analysis shown in Figure 2.

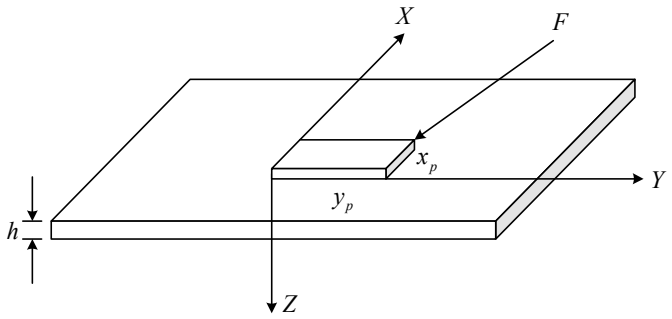

Figure 2: Force analysis of the force measuring plate

The geometric center of the surface of the force plate is the origin of the coordinate system, the positive direction of the Y-axis is opposite to the junction, the positive direction of the X-axis is to the left when viewed in the direction of the Y-axis, and the positive direction of the z-axis is to the downward direction as determined by the right-hand rule. p is the center of plantar pressure and h is the thickness of the material covering the surface of the force plate.

The product of the 6-channel voltage outputs $(V_1 - V_6)$ and their corresponding gain scaling factors $(C_1 - C_6)$ is used to express the 6 load components of the force plate, i.e., the force of the force plate in the X, Y, Z direction (F_X, F_Y, F_Z) and moment (M_X, M_Y, M_Z) as shown in Eq. (16), and the position of plantar force center point is calculated by Eq. (17).

$$\begin{aligned} F_X &= C_1 \times V_1 \quad F_Y = C_2 \times V_2 \quad F_Z = C_3 \times V_3 \\ M_X &= C_4 \times V_4 \quad M_Y = C_5 \times V_5 \quad M_Z = C_6 \times V_6 \end{aligned} \tag{16}$$

$$\begin{aligned} x_p &= \frac{-h \cdot F_X - M_Y}{F_Z} \\ y_p &= \frac{-h \cdot F_Y + M_X}{F_Z} \end{aligned} \tag{17}$$

III. Computer-aided modeling of the biomechanical characteristics of the lower extremity in jumping sports

A total of 100 test subjects were recruited for this study, and 87 subjects were selected after screening to carry out the experiment. The inclusion criteria of the test subjects: (1) no sports injury within six months; (2) normal gait, normal movement of each joint; (3) no other health diseases, no drug dependence; (4) all the data obtained from the test can be used normally; and (5) the subjects and their parents agreed to and signed the Volunteer Informed Consent Form. Prior to the start of the study, all subjects signed the volunteer consent form and were informed about the entire testing process. For the purpose of the later study, the jumping situation was divided into two categories according to the performance evaluation criteria, and those who achieved a good situation were classified as Group I (56) and the rest as Group II (31).

III. A. Model validation

III. A. 1) Comparative validation of kinematic data

Visual3D software is commonly used in sports biomechanics research for kinematic data and kinetic data calculation, this calculation is based on the laboratory measured Marker point coordinate data and the ground reaction force measured by the force platform, which is a reproduction of the motion state, and is a recognized and reliable calculation. Taking the knee angle change data as a sample, the V3D results were compared with the OpenSim simulation results for similarity within the ICC group, and the knee angle comparison validation results are shown in Figure 3. The principle of kinematics and dynamics data obtained from inverse kinematics and inverse dynamics solving of OpenSim model is consistent with that of Visual3D, and the degree of consistency of the results obtained from the two calculations, to a certain extent, can prove the reliability of OpenSim simulation calculations. By validating the ICC intra-group similarity of the kinematic data of the two groups at the same time stage, the correlation coefficient was 0.915, with a p-value of less than 0.001, which is a significant difference. It can show the high similarity between the two, thus proving the reliability of the model.

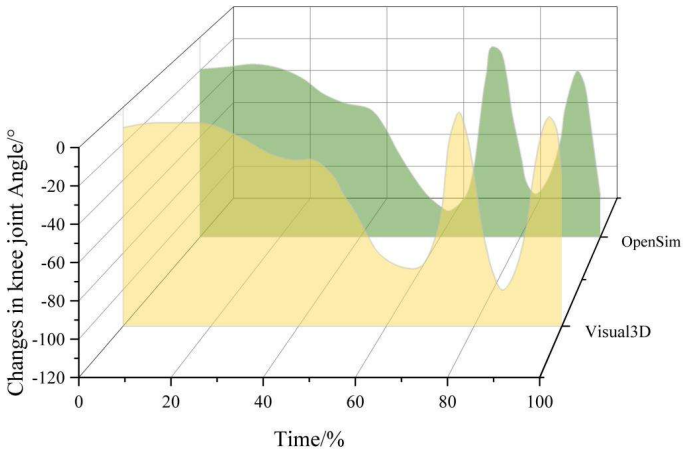

Figure 3: Comparison and verification results of knee joint angles

III. A. 2) Surface EMG Verification

The EMG data were preprocessed using Visual3D, sequentially performing a 4th order 50 Hz high-pass filtering process, full-wave rectification, a 4th order 20 Hz low-pass filtering process to produce a linear envelope, and then the EMG signals were scrutinized visually. The presence of high-frequency noise interference in the signal was processed using a lower frequency low-pass filter. The linear envelope of the EMG was then normalized using the amplitude maximum of the block of muscle during the action cycle, and finally the linear envelope was normalized to 101 data points from the beginning to the end of the action and the data was saved as a file in CSV format.

In OpenSim, a specific action phase was selected, and Scale scaling, K inverse kinematics ID inverse dynamics, and SO optimization analysis were run sequentially to obtain the muscle activation changes during jumping, and the data of the right rectus femoris muscle was selected, and it was subjected to intra-group similarity analysis with the rectus femoris muscle signals after envelopment, and the results of the comparison of EMG linear envelope and OpenSim muscle activation are shown in Fig. 4. It can be seen that the two are highly similar (P<0.001), proving the reliability of the model.

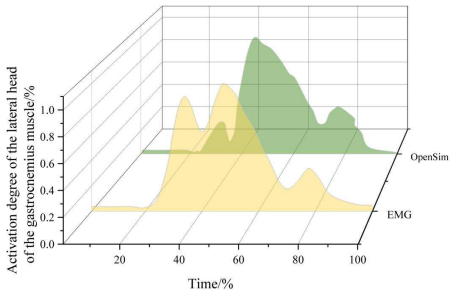

Figure 4: Comparison results of electromyography and OpenSim

III. B. Analysis of Biomechanical Indicators of Jumping

III. B. 1) Kinematic analysis

The results of the comparison of the changes in knee joint angle and angular velocity between group I and group II and the results of SPM_1d test are shown in Figures 5 and 6, respectively. There was a significant difference in knee joint angle between group I and group II at 35%-55% of the action cycle (t=2.846, P<0.001), and at 65%-70% of the action cycle (t=2.947, P<0.05).The knee joint Angular velocity was significantly significantly different at 25%-29% of the movement cycle (t=2.597, P<0.05) and at 57%-63% of the movement cycle (t=2.946, P<0.001).

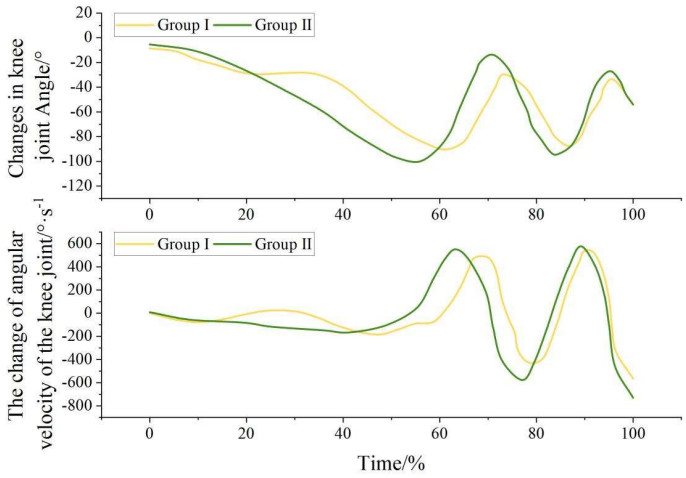

Figure 5: Comparison results of knee joint Angle and angular velocity changes

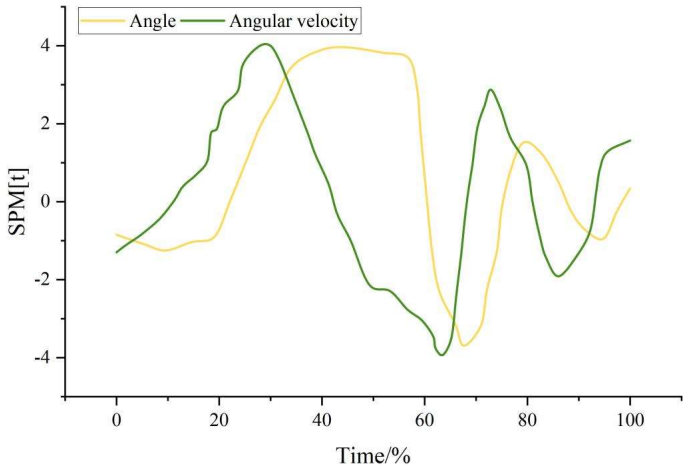

Figure 6: Test results of SPM_1D

III. B. 2) Muscle electrical signals

For the electromyographic analysis of the lower limb from the starting stirrup to the landing, the muscles selected were the tibialis anterior, medial head of gastrocnemius, rectus femoris, and long head of the biceps femoris of the supporting leg. A typical representative of each of the two groups was selected from Group I and Group II, and the electromyographic values of each muscle of the lower limb are shown in Fig. 7(a~b), respectively. In both groups, the tibialis anterior and rectus femoris muscles of the supporting leg were the first to exert force, and these two active muscles provided the main power for the stirrup extension in the jumping phase. The gastrocnemius and biceps femoris, which are the antagonist muscles, start to fire later, but there is still a big difference between the two groups: the antagonist muscles in group I are in a state of very low firing during the jump, and they are almost completely relaxed until they are converted into the active muscles during the landing, whereas all the four muscles in group II have a big discharge in the jump, which indicates that the lower limb is in a very tense and uncoordinated state.

By analyzing and processing the raw EMG signals, the muscles that fired the most during the jump in group I were the tibialis anterior and rectus femoris, and the medial head of gastrocnemius and the long head of biceps

femoris fired less. In group II, the medial head of gastrocnemius and rectus femoris had the highest force during the jump, followed by the tibialis anterior and the long head of the biceps femoris, and the smallest was the long head of the biceps femoris. In group I, the muscles of the supporting leg were sufficiently strong and coordinated, and the jumping stirrups were smooth and powerful. In group II, there was an obvious pause before the jump, and the overall rhythm of the jump was not well grasped. The excessive tension of the supporting leg muscles was one of the main reasons for the poor jumping effect.

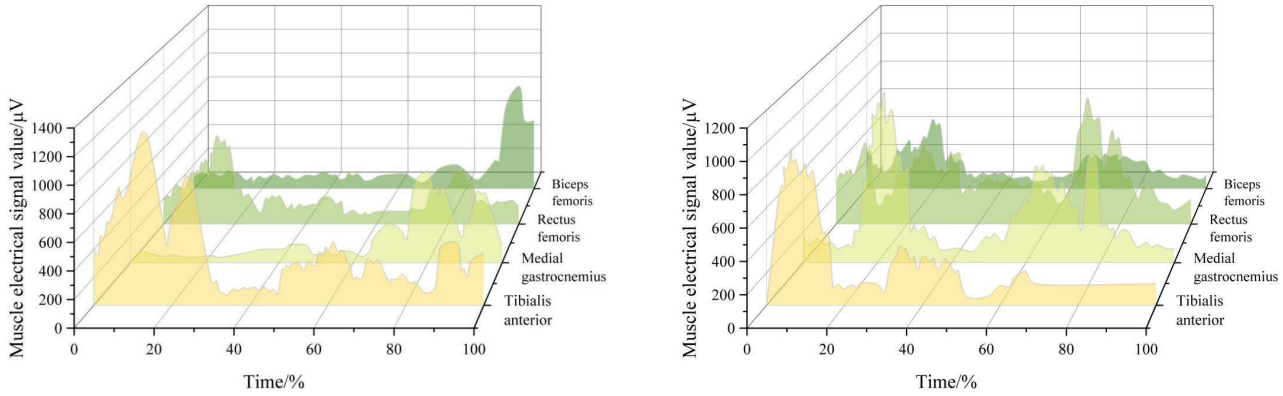

(a) Representative of Group I (b) Representative of Group Ⅱ

Figure 7: Electromyographic values of each muscle in the lower extremities

III. B. 3) Analysis of center of mass displacement parameters

Three representatives of each group were selected, and the displacement of center of mass and the comparison of the vacating time during the jumping process are shown in Table 1. The vacating time of the representatives of group I is more than 0.7 s, and the displacement of Z-axis in vertical direction is more than 0.7 m. The displacement of Z-axis and the corresponding vacating time of representatives of group I are higher than that of representatives of group II. When the human body is vacated, the external force is only gravity (air resistance is ignored), from the free-fall formula and then according to the law of conservation of mechanical energy, it is further confirmed that the Z-axis displacement is determined by the initial velocity in the Z-axis direction given at the time of jumping, i.e., the larger the vertical velocity is at the time of jumping, the larger the height of the vacated height is, and the longer the time of vacating is. The horizontal velocity accumulated during the straight line gliding is the basis of the velocity at the jump, while the full utilization of the rapid force in the stomping and reaching phase to maximize the upward velocity of the body is the key technical link.

Table 1: Comparison of centroid displacement(m) and idle time(s)

Parameters	Group I				Group Ⅱ			
	I1	I2	I3	M±SD	Ⅱ1	Ⅱ2	Ⅱ3	M±SD
X-axis displacement	2.55	2.57	2.68	2.60±0.07	2.69	2.71	2.22	2.54±0.28
Y-axis displacement	2.84	2.38	2.01	2.41±0.42	1.47	1.75	1.74	1.65±0.16
Z-axis displacement	0.71	0.75	0.74	0.73±0.02	0.61	0.55	0.48	0.55±0.07
Resultant displacement	3.06	2.88	3.15	3.03±0.14	3.24	2.98	2.65	2.96±0.30
Time to empty	0.76	0.73	0.71	0.73±0.03	0.61	0.53	0.64	0.59±0.06

IV. Conclusion

In this paper, computer-aided modeling was used to analyze the biomechanical properties of the lower limbs in jumping exercise.

(1) There was a significant difference in knee angle between group I and group II at 35%-55% of the action cycle ($t=2.846$, $P<0.001$), and at 65%-70% of the action cycle ($t=2.947$, $P<0.05$.) There was a significant difference in knee angular velocity at 25%-29% of the action cycle ($t=2.597$, $P<0.05$), and at 57%-63% of the movement cycle there was a significant difference ($t=2.946$, $P<0.001$).

(2) The muscles that exerted the most force during the jump in group I were the tibialis anterior and rectus femoris, with less force exerted by the medial head of the gastrocnemius and the long head of the biceps femoris. In group II, the medial head of gastrocnemius and rectus femoris had the highest force during the jump, followed by the tibialis anterior and the long head of the biceps femoris, and the smallest was the long head of the biceps femoris. The supporting leg muscles of group I were sufficiently strong and coordinated, and the jumping stirrups were smooth and powerful. In group II, there was an obvious pause before the jump, and the overall rhythm of the jump was not well grasped. The excessive tension of the supporting leg muscles was one of the main reasons for the poor jumping effect.

(3) Representatives of Group I had an airtime of more than 0.7s, and the displacement in the vertical direction of the Z-axis was more than 0.7 m. The displacement in the direction of the Z-axis and the corresponding airtime of representatives of Group I were higher than those of representatives of Group II. The horizontal speed accumulated in the straight line gliding is the basis of the jumping speed, and it is the key technical link to fully utilize the fast power in the stomping and reaching phase to make the body obtain the maximum upward speed.

References

[1] Saadat, S., Stephenson, M. L., & Gillette, J. C. (2024). Entry angle during jump landing changes biomechanical risk factors for ACL injury. Sports Biomechanics, 23(12), 3090-3102.

[2] Lopes, T. J. A., Simic, M., Myer, G. D., Ford, K. R., Hewett, T. E., & Pappas, E. (2018). The effects of injury prevention programs on the biomechanics of landing tasks: a systematic review with meta-analysis. The American journal of sports medicine, 46(6), 1492-1499.

[3] Yang, C., Yao, W., Garrett, W. E., Givens, D. L., Hacke, J., Liu, H., & Yu, B. (2018). Effects of an intervention program on lower extremity biomechanics in stop-jump and side-cutting tasks. The American journal of sports medicine, 46(12), 3014-3022.

[4] Zhou, H., Xu, D., Chen, C., Ugbolue, U. C., Baker, J. S., & Gu, Y. (2021). Analysis of different stop-jumping strategies on the biomechanical changes in the lower limbs. Applied Sciences, 11(10), 4633.

[5] Zhao, P., Ji, Z., Wen, R., Li, J., Liang, X., & Jiang, G. (2021). Biomechanical characteristics of vertical jumping of preschool children in China based on motion capture and simulation modeling. Sensors, 21(24), 8376.

[6] Radakovic, R., & Filipovic, N. (2020). Sport biomechanics: Experimental and computer simulation of knee joint during jumping and walking. In Computational Modeling in Bioengineering and Bioinformatics (pp. 387-418). Elsevier.

[7] Martinez, C. M., & Wainwright, P. C. (2019). Extending the geometric approach for studying biomechanical motions. Integrative and Comparative Biology, 59(3), 684-695.

[8] Caruntu, D. I., & Moreno, R. (2019). Human knee inverse dynamics model of vertical jump exercise. Journal of Computational and Nonlinear Dynamics, 14(10), 101005.

[9] Li, J., & Du, H. (2020). Research on the sports biomechanics modeling of the human motion technical movements. In Cyber Security Intelligence and Analytics (pp. 243-248). Springer International Publishing.

[10] Olberding, J. P., Deban, S. M., Rosario, M. V., & Azizi, E. (2019). Modeling the determinants of mechanical advantage during jumping: consequences for spring-and muscle-driven movement. Integrative and Comparative Biology, 59(6), 1515-1524.

[11] Qian, J., Mao, Y., Tang, X., Li, Z., Wen, C., & Zhang, S. (2020). A finite element model for estimation of contact dynamics during a jumping movement on a trampoline. Journal of human kinetics, 73, 59.

[12] Dehaghani, M. R., Nourani, A., & Arjmand, N. (2022). Effects of auxetic shoe on lumbar spine kinematics and kinetics during gait and drop vertical jump by a combined in vivo and modeling investigation. Scientific Reports, 12(1), 18326.

[13] Lin, Y., Lu, Z., Cen, X., Thirupathi, A., Sun, D., & Gu, Y. (2022). The influence of different rope jumping methods on adolescents' lower limb biomechanics during the ground-contact phase. Children, 9(5), 721.

[14] Lu, Y., Wang, H., Qi, Y., & Xi, H. (2021). Evaluation of classification performance in human lower limb jump phases of signal correlation information and LSTM models. Biomedical Signal Processing and Control, 64, 102279.

[15] Keogh, J. A., Waddington, E. E., Masood, Z., Mahmood, S., Palanisamy, A. C., Ruder, M. C., ... & Kobsar, D. (2023). Monitoring lower limb biomechanical asymmetry and psychological measures in athletic populations—A scoping review. Scandinavian Journal of Medicine & Science in Sports, 33(11), 2125-2148.

[16] Silva, M., Freitas, B., Andrade, R., Carvalho, Ó., Renjewski, D., Flores, P., & Espregueira-Mendes, J. (2021). Current perspectives on the biomechanical modelling of the human lower limb: a systematic review. Archives of Computational Methods in Engineering, 28, 601-636.

[17] Zhao, P., Ji, Z., Wen, R., Li, J., Liang, X., & Jiang, G. (2021). Biomechanical characteristics of vertical jumping of preschool children in China based on motion capture and simulation modeling. Sensors, 21(24), 8376.

[18] Cabarkapa, D., Fry, A. C., Cabarkapa, D. V., Myers, C. A., Jones, G. T., Philipp, N. M., ... & Deane, M. A. (2022). Differences in biomechanical characteristics between made and missed jump shots in male basketball players. Biomechanics, 2(3), 352-360.

[19] Bulat, M., Can, N. K., Arslan, Y. Z., & Herzog, W. (2019). Musculoskeletal simulation tools for understanding mechanisms of lower-limb sports injuries. Current Sports Medicine Reports, 18(6), 210-216.

[20] Pedley, J. S., Lloyd, R. S., Read, P. J., Moore, I. S., De Ste Croix, M., Myer, G. D., & Oliver, J. L. (2020). Utility of kinetic and kinematic jumping and landing variables as predictors of injury risk: a systematic review. Journal of Science in Sport and Exercise, 2, 287-304.